

## **Phospholipid dependent mechanism of smp24, an $\alpha$ -helical antimicrobial peptide from scorpion venom**

HARRISON, Patrick L., HEATH, George R., JOHNSON, Benjamin R.G., ABDEL-RAHMAN, Mohamed A., STRONG, Peter, EVANS, Stephen D. and MILLER, Keith <<http://orcid.org/0000-0001-8633-6952>>

Available from Sheffield Hallam University Research Archive (SHURA) at:

<http://shura.shu.ac.uk/13217/>

---

This document is the author deposited version. You are advised to consult the publisher's version if you wish to cite from it.

### **Published version**

HARRISON, Patrick L., HEATH, George R., JOHNSON, Benjamin R.G., ABDEL-RAHMAN, Mohamed A., STRONG, Peter, EVANS, Stephen D. and MILLER, Keith (2016). Phospholipid dependent mechanism of smp24, an  $\alpha$ -helical antimicrobial peptide from scorpion venom. *Biochimica et Biophysica Acta (BBA) - Biomembranes*, 1858 (11), 2737-2744.

---

### **Copyright and re-use policy**

See <http://shura.shu.ac.uk/information.html>



# Phospholipid dependent mechanism of smp24, an $\alpha$ -helical antimicrobial peptide from scorpion venom

Patrick L. Harrison<sup>a</sup>, George R. Heath<sup>b</sup>, Benjamin R.G. Johnson<sup>b</sup>, Mohamed A. Abdel-Rahman<sup>a,c</sup>, Peter N. Strong<sup>a</sup>, Stephen D. Evans<sup>b</sup>, Keith Miller<sup>a,\*</sup>

<sup>a</sup> Biomolecular Research Centre, Sheffield Hallam University, Sheffield, UK

<sup>b</sup> Department of Physics and Astronomy, Leeds University, Leeds, UK

<sup>c</sup> Zoology Department, Faculty of Science, Suez Canal University, Ismailia 41522, Egypt

## ARTICLE INFO

### Article history:

Received 1 April 2016

Received in revised form 6 July 2016

Accepted 27 July 2016

Available online 30 July 2016

### Keywords:

Antimicrobial peptides

Membrane damage

Atomic force microscopy

Quartz crystal microbalance-dissipation

## ABSTRACT

Determining the mechanism of action of antimicrobial peptides (AMPs) is critical if they are to be developed into the clinical setting. In recent years high resolution techniques such as atomic force microscopy (AFM) have increasingly been utilised to determine AMP mechanism of action on planar lipid bilayers and live bacteria. Here we present the biophysical characterisation of a prototypical AMP from the venom of the North African scorpion *Scorpio maurus palmatus* termed Smp24. Smp24 is an amphipathic helical peptide containing 24 residues with a charge of +3 and exhibits both antimicrobial and cytotoxic activity and we aim to elucidate the mechanism of action of this peptide on both membrane systems.

Using AFM, quartz crystal microbalance-dissipation (QCM-D) and liposomal leakage assays the effect of Smp24 on prototypical synthetic prokaryotic (DOPG:DOPC) and eukaryotic (DOPE:DOPC) membranes has been determined. Our data points to a toroidal pore mechanism against the prokaryotic like membrane whilst the formation of hexagonal phase non-lamellar phase structures is seen in eukaryotic like membrane. Also, phase segregation is observed against the eukaryotic membrane and this study provides direct evidence of the same peptide having multiple mechanisms of action depending on the membrane lipid composition.

© 2016 The Authors. Published by Elsevier B.V. This is an open access article under the CC BY-NC-ND license (<http://creativecommons.org/licenses/by-nc-nd/4.0/>).

## 1. Introduction

Antimicrobial peptides (AMPs) are essential contributors to the innate immune system and are found among all biological classes. Over one thousand AMPs have been discovered and biologically characterised to date, although the mechanism(s) by which the vast majority of these peptides function is not fully understood. The membrane-disruptive effects of AMPs are well established with three main mechanisms proposed, namely the barrel stave, toroidal pore and carpet models [1]. For each of these mechanisms the key factor for membrane disruption is the initial electrostatic attraction of the peptide to the negatively charged bacterial membrane surface [2,3]. In all cases, following initial electrostatic attraction, a threshold concentration must be realized before membrane disruption can occur [2,4]. In the barrel stave mechanism a central lumen forms within the pore as a result of peptide oligomerisation [5]. AMPs bind as a monomer and adopt an  $\alpha$  helical secondary structure inducing localised membrane thinning by sitting at the phospholipid chain/head group interface, upon the threshold concentration being reached the hydrophobic face inserts into the membrane core and the peptides begin to self associate [6]. In the toroidal mechanism the pore lumen is lined by both peptide

and lipid head group interactions and is characterised by the induction of membrane curvature due to interaction of the hydrophilic face of the peptide with polar head groups, this causes bending of the head groups in a continuous fashion to connect the outer and inner membrane leaflet due to the thermodynamically unfavourable interaction between the acyl chain and the aqueous environment [7]. In the carpet model [3] the peptides cover the membrane surface and, upon the threshold concentration being reached, form transient pores allowing peptide access to the inner leaflet leading to peptide carpet formation on each membrane surface. Peptides can then span the transmembrane bilayer causing curvature of the membrane to protect the acyl chains which leads to the disintegration of the bilayer due to micelle formation. Recent models however, have blurred the lines between these three alternatives. While these mechanisms are still the most frequently proposed, a number of other mechanisms have emerged including the interfacial, leaky slit, aggregate, electroporation, sinking raft, and lipid aggregate models (see [2] for an extensive review).

Due to the fundamental role cellular membranes play in the regulation and function of all cells, it is critical for the clinical introduction of AMPs that we understand the precise mechanisms by which they interact with both prokaryotic and eukaryotic membranes. Previous mechanistic studies have focused on the lytic effect of AMPs on liposomes [8,9]; while this has been valuable in determining the propensity

\* Corresponding author.

E-mail address: [K.miller@shu.ac.uk](mailto:K.miller@shu.ac.uk) (K. Miller).

of a peptide to damage a cell membrane and cause cell death, it does not inform us of non-lytic effects and membrane structural changes that could be occurring.

Atomic force microscopy (AFM) has become an established technique to image planar lipid bilayers [10]; however it has only recently been employed to determine the mechanism of action of AMPs [11–15]. A major advantage of AFM over other biophysical techniques is that it allows nano-scale visualisation of an AMP's effects on a membrane in a pseudo-native state, thereby offering an unparalleled insight into any membrane changes that may be induced.

Scorpion venoms are a rich source of antimicrobial peptides [16,17]. In this study we have examined the mechanism of action of Smp24 (24 amino acids, charge +3), a prototypical amphipathic AMP that was identified by genomic analysis of *Scorpio maurus palmatus* [18]. Previous CD analysis determined Smp24 to be unordered in aqueous solution but adopts an  $\alpha$ -helical structure in the presence of 60% TFE with two helical regions of approximately 59% and 22% predicted [19]. We have used AFM and quartz crystal microbalance-dissipation (QCM-D) to study the effects of Smp24 on hydrated lipid membranes, in addition to liposome leakage assays. Our results show that Smp24 has multiple modes of action, depending on lipid composition. This study highlights the need for advanced biophysical analysis of the action of AMPs against a variety of different membrane compositions. At the present moment, cell lysis is the primary measurable endpoint of AMP action. We expect our approach will diversify our knowledge and understanding of membrane targets, by increasing the range of outputs by which AMP action can be evaluated.

## 2. Materials and methods

### 2.1. Materials

Smp24 (96.2% pure) was synthesised using solid-phase chemistry and was purchased from Think Peptides (Oxford, UK). Carboxyfluorescein was purchased from Sigma (Gillingham, UK) and all solvents other reagents were of the highest grade available and were obtained from Sigma (Gillingham, UK). Phospholipids 1,2-dioleoyl-*sn*-glycero-3-phosphoethanolamine (DOPE-18:1 ( $\Delta 9$ -Cis), 1,2-dioleoyl-*sn*-glycero-3-phospho-(1'-*rac*-glycerol) (DOPG-16:0), 1,2-dioleoyl-*sn*-glycero-3-phosphocholine (DOPC-18:1 ( $\Delta 9$ -Cis) and 1',3'-bis[1,2-dimyristoyl-*sn*-glycero-3-phospho]-*sn*-glycerol (Cardiolipin-14:0) were purchased from Avanti Polar Lipids (Alabaster, AL).

### 2.2. AFM imaging of hydrated lipid bilayers

Supported planar lipid bilayers were produced on a freshly cleaved mica surface by vesicle rupture using tip sonicated vesicles incubated on the mica at a concentration of 0.5 mg/mL (as described by [20]). For bilayers containing negatively charged lipids 2 mM  $\text{CaCl}_2$  was added to the lipid mixture just before incubation on the surface. After 20 min incubation the surface was rinsed at least 10 times to remove vesicles from the bulk phase. The presence of a uniform bilayer was confirmed by lateral scanning in tapping mode over a  $64 \mu\text{m}^2$  area and the presence of multiple bilayers was ruled out by a statistically significant (nine) number of force spectroscopy curves. Observations of the attack of Smp24 were performed using a Nanoscope IIIa Multimode atomic force microscope (Digital instruments Santa Barbara CA).

### 2.3. QCM-D protocol

QCM-D measurements were performed using a QSense E4 multifrequency QCM-D instrument (Q-Sense, Gothenburg, Sweden) in a flow through cell of 40  $\mu\text{L}$  volume. Data from 15, 25, 35, 45, 55, and 65 MHz overtones (3rd, 5th, 7th, 9th, 11th, and 13th respectively) were collected. Before use, all  $\text{SiO}_2$  crystals were cleaned by ultrasonication in 0.4% SDS for 15 min followed by copious rinsing and ultrasonication in

water for 15 min. The crystals were then dried under nitrogen and UV-ozone cleaned for 20 min. After UV-ozone treatment, they were rinsed with water, dried under nitrogen, and used immediately. Experiments were performed at 22 °C. Lipid vesicles were injected at a concentration of 0.5 mg/mL to form the bilayer. After rinsing successive peptide concentrations (0.2–2.0  $\mu\text{M}$ ) were injected at a flow rate of 50  $\mu\text{L}/\text{min}$ . Changes in dissipation and normalised frequency were monitored for a period of 20 mins before the next injection. Changes in the dissipation ( $D$ ), and normalised frequency ( $f$ , where  $f = f_n/n$  and  $n$  is the number of the overtone, i.e.  $n = 3, 5, 7$  etc.) of the 5th overtone ( $n = 5, 25 \text{ MHz}$ ) are presented.

### 2.4. Liposome leakage assay

Liposomes were made using an extruder method with lipids at a concentration of 0.5 mg/mL [20]. Liposome release assays using carboxyfluorescein (CF) were performed as follows: peptide sample (20  $\mu\text{L}$ ), liposomes (10  $\mu\text{L}$ ) and buffer (50 mM sodium phosphate, 10 mM NaCl and 1 mM of ethylenediaminetetraacetic acid (EDTA) pH 7.4) (170  $\mu\text{L}$ ) were incubated in the dark for 15 min. Fluorescence (480/520 nm) was measured on a Tecan infinite M200 plate reader (Tecan, UK). The reaction mix without CF was used as a negative control to normalise results and 10% Triton-X was used as a positive control to measure complete dye release. The rate of CF leakage was expressed as the percentage of dye released of the total encapsulated carboxyfluorescein and then normalised against the blank buffer signal. All samples were run in triplicate.

## 3. Results

### 3.1. Analysis of Smp24 using liposome leakage assays

Liposome leakage assays were performed on a number of different liposome compositions (Fig. 1).

Against a negatively charged PCPG (1:1) (phosphocoline: phosphoglycerol) composition, significant membrane disruption occurred at an AMP concentration of 1.25  $\mu\text{M}$  with 37.7% ( $\pm 1.7$ ) CF release observed and 70.9% ( $\pm 2.6$ ) leakage seen when the AMP concentration was increased to 2  $\mu\text{M}$ . The electrostatic nature of this attack has also been examined with a decrease in CF release in the presence of 500 mM NaCl, only 6.25% ( $\pm 1.0$ ) at an AMP concentration of at 1.25  $\mu\text{M}$  and 53.3% ( $\pm 2.19$ ) at 2  $\mu\text{M}$  AMP was observed.

Against the neutrally charged PCPE (1:1) (phosphocoline: phosphoethanolamine) composition, CF release is less pronounced with 19.6% ( $\pm 1.7$ ) observed at 1.25  $\mu\text{M}$  peptide concentration with a gradual increase in leakage to 48.7% ( $\pm 2.0$ ) at 2  $\mu\text{M}$ . However any membrane disruptive effects are not electrostatically driven with no significant difference in lyses observed in the presence of salt.

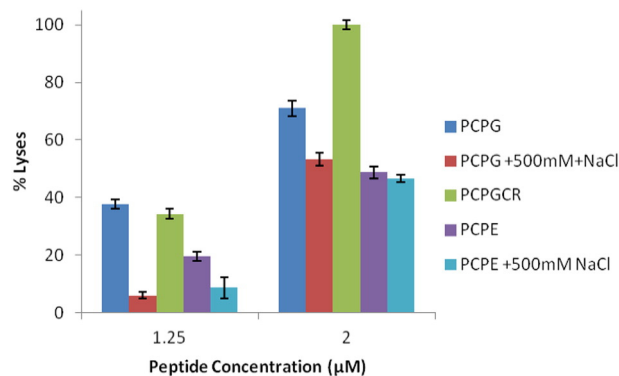


Fig. 1. The effect of Smp24 on a number of different membrane compositions at both 1.25 and 2  $\mu\text{M}$  peptide concentration (Error bars  $\pm$  SD).

The inclusion of 10% cardiolipin, common in bacterial membranes, increased leakage at 1.25  $\mu\text{M}$  Smp24 (PC:PG:CR 45:45:10) when compared with the CR deficient liposomes, with maximum release seen at 1.75  $\mu\text{M}$  and above.

### 3.2. Analysis of Smp24 attack on hydrated lipid bilayers using AFM

AFM was used to visualize hydrated lipid bilayers following AMP attack with Smp24 (0.4–2.0  $\mu\text{M}$ ) against both PC:PG, PC:PE and a bilayer that exhibits phase separation. Both the PC:PG and PC:PE compositions were chosen as model membrane compositions to represent prototypical

membranes of prokaryotic and eukaryotic membranes respectively and sphingomyelin (SM) was incorporated to induce phase separation.

The PC:PG bilayer exhibited a smooth appearance before peptide attack with no visible defects (Fig. 2A), AFM force spectroscopy was used to confirm the existence of a bilayer as previously shown [20]. Pore formation was seen after treatment with Smp 24 over a concentration range of 0.4–1.25  $\mu\text{M}$  (Fig. 2B). After 30 min incubation pore size remained stable over time with diameters ranging between 20 and 150 nm with an average of  $80 \pm 40$  nm (sd) (Fig. 2C). As shown by Fig. 2D the pore depths were typically 2–4 nm. Increased peptide concentration (2.0  $\mu\text{M}$ ) caused the complete destruction of the bilayer in

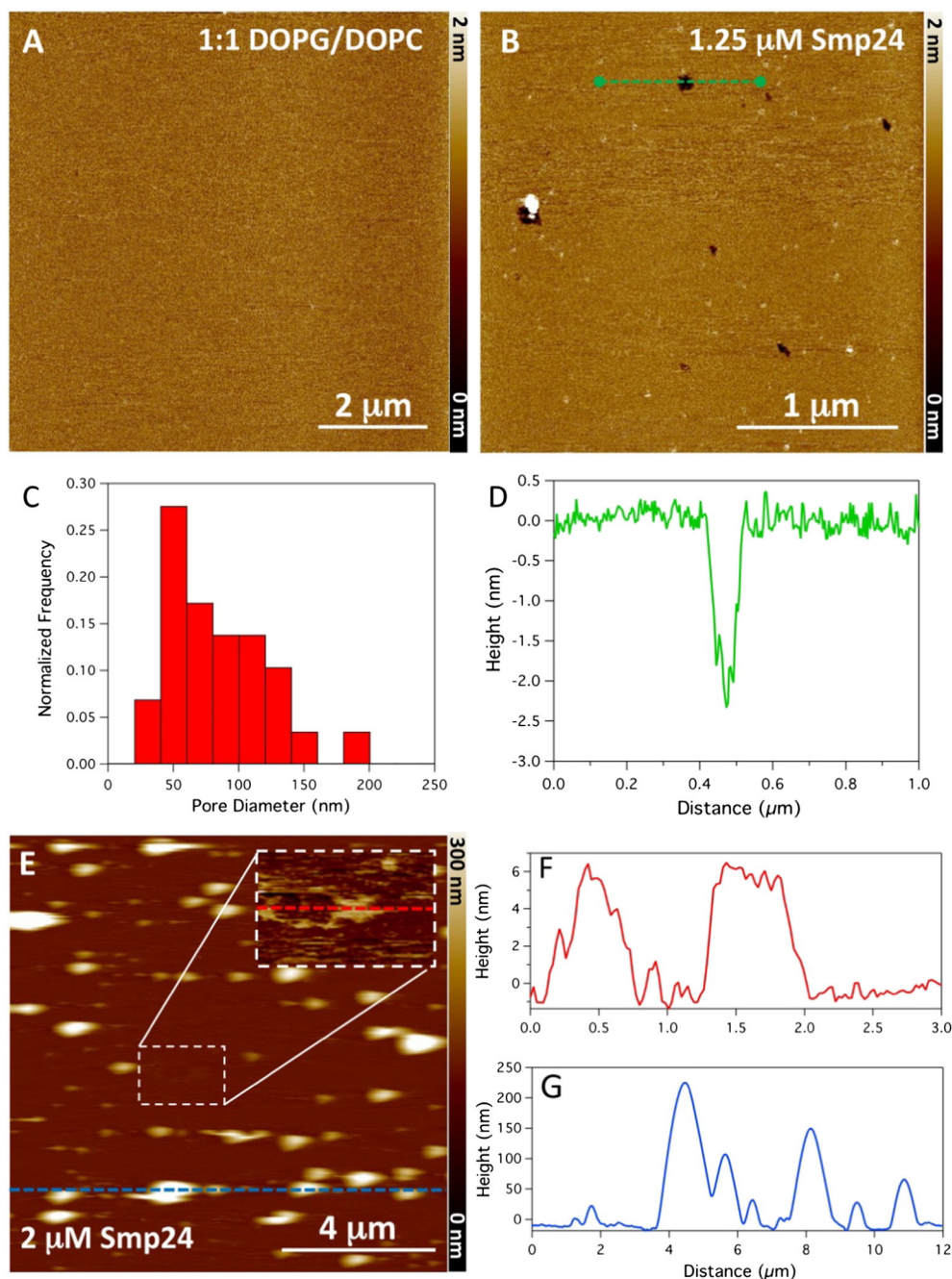


**Fig. 2.** The effect of Smp24 against negatively charged (1:1) PC:PG membranes at various peptide concentrations. (A): The PC:PG bilayer before Smp24 incubation, (B): Pore formation with the PCPG bilayer after incubation with 1.25  $\mu\text{M}$  Smp24, (C): Histogram showing the distribution of detectable pore sizes after incubation with 1.25  $\mu\text{M}$  Smp24 ( $n = 29$ ), (D): Line profile across pore in image (B) showing the typical depth of the pores. (E): Complete disruption of a PCPG bilayer after incubation with 2  $\mu\text{M}$  Smp24 with inset showing remaining bilayer patch, (F) and (G) line profiles across areas of image (E) showing the heights of surface vesicles and membrane patches respectively.



5 mins. As can be seen in Fig. 2E, a small number of fragments of bilayer, ~6 nm high, are still on the mica surface (Fig. 2F) whilst the rest of the surface is either clear or has large 50–200 nm vesicles attached to it (Fig. 2G).

Following exposure of a PC:PE bilayer to 1.25  $\mu\text{M}$  Smp24 no pore formation is observed; removal of the bilayer in stratified lines is seen instead (Fig. 3A–C), with the disrupted areas approximately 200 nm wide, to a depth of 0.3–0.5 nm (Fig. 3D). Addition of higher peptide concentrations (2.0  $\mu\text{M}$ ) to PC:PE bilayers resulted in increased disruption. After 5 min incubation the PC:PE bilayer has fewer defects which larger size compared to the same bilayer with 1.25  $\mu\text{M}$  Smp24 (Fig. 3A, E). Over time the shallow defects (0.5 nm) develop further holes which have depths of 4 nm (Fig. 3G,H). The inclusion of 10% Cholesterol into the PC:PG lipid mixture showed similar effects of Smp24 attack to that of the PC:PE membranes. At 1.25  $\mu\text{M}$  Smp24 thinning defects (~0.3 nm deep) appear within 5 min peptide incubation (Fig. 3I), after 15 min (Fig. 3J, K) these defects increase in depth to 1 nm (Fig. 3L) with some areas showing complete membrane removal (~4–5 nm deep defects).

A phase separated bilayer (60% DOPC, 20% Sphingomyelin, 20% Cholesterol) was chosen as a way of investigating the effect of peptide attack on coexisting lipid domains. Before peptide addition, Fig. 4 at 0 s, lipid ordered ( $L_o$ ) domains (0.6–0.9 nm high) are observed surrounded by a lipid disordered ( $L_d$ ) phase, seen with the lighter coloured areas being the  $L_o$  phase. After exposing bilayers to 1.0  $\mu\text{M}$  peptide (a concentration to determine the effect on membranes without causing pore formation), the  $L_o$  domains reshape and reorganize over time, with some merging into larger domains whilst others break up into smaller domains. This increase in dynamics combined with the resulting domains having increased domain perimeter implies a reduction in the domain interfacial line tension [21]. Analysing the area/perimeter ratio provides a quantitative measure which can be directly related to the line tension [22]. Performing this analysis (Fig. 4) on single domains (excluding

domains which merge or break up) clearly shows how the line tension dramatically decreases over time, reaching a steady state after 25 min.

### 3.3. Analysis of Smp24 attack on hydrated lipid bilayers using QCM-D

QCM-D curves for PC:PG and PC:PE bilayers after peptide attack with consecutively increasing concentrations are shown in Fig. 5A & B respectively. In each graph the frequency has been inverted, with a decrease in frequency representative of an increased peptide accumulation.

At low concentrations of Smp24 (0.1–0.2  $\mu\text{M}$ ) acting on PC:PG bilayers, the frequency decreases (–24 Hz to –25.5 Hz) with an increase in dissipation (0.2 to 0.35). Increasing peptide concentration to 0.75  $\mu\text{M}$  initially results in large changes in both frequency (to –37.3 Hz) and dissipation (to 1.6); however, dissipation then falls away to 1.4. This “swing back” phenomenon could represent a threshold concentration being overcome and membrane incursion subsequently taking place. A further injection of 0.75  $\mu\text{M}$  peptide has little observed effect. Interestingly an increase to 1.25  $\mu\text{M}$  peptide further decreases frequency (to –45 Hz) and but significantly increases dissipation again (to 2.8), possibly reflecting further peptide accumulation and further incursion into the membrane. In contrast, when PC:PE bilayers are exposed to similarly increasing concentrations of smp24, there is an overall increase in frequency (–27.7 Hz to –24.4 Hz) and a minor decrease in dissipation (0.66 to 0.44). The lack of dissipation “swing back” would also suggest that a threshold accumulation and incursion event does not take place on PC:PE bilayers as no transient stabilisation of the bilayer is seen expected after initial peptide insertion.

## 4. Discussion

Prokaryotic membranes are more negatively charged than their eukaryotic counterparts, due to an increased presence of the hydroxylated

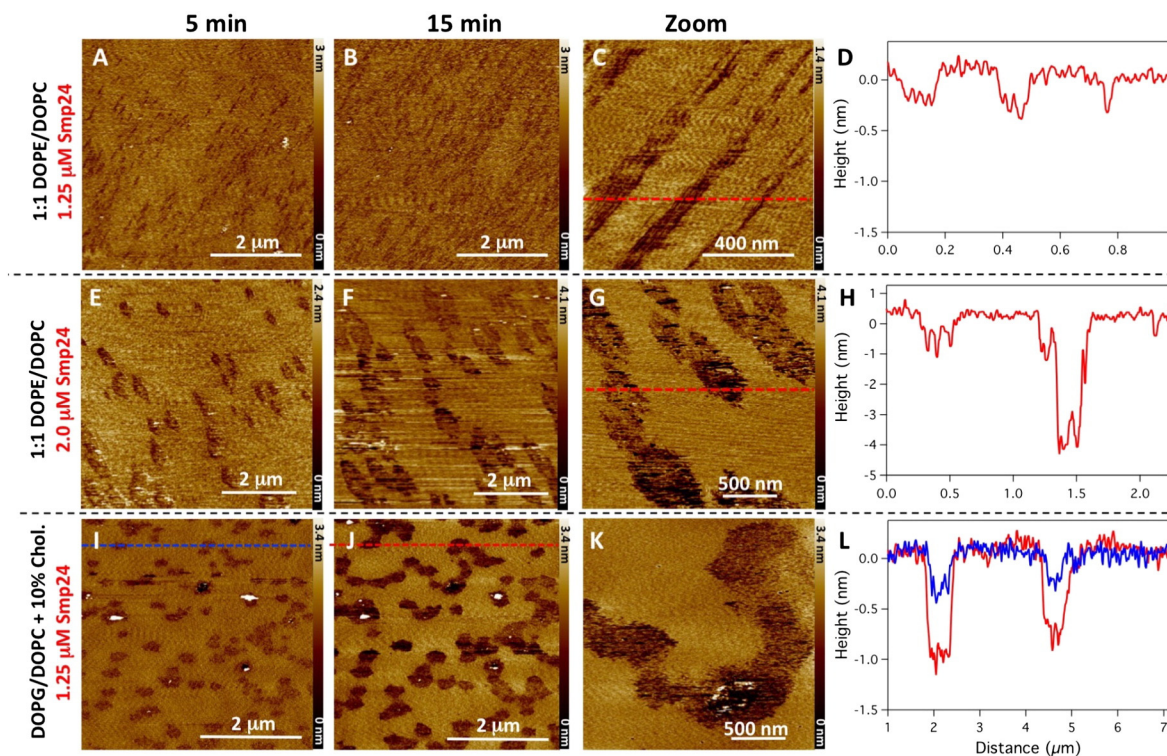


**Fig. 3.** AFM images showing the effect of Smp24 on PC:PE (1:1) bilayers (1.25  $\mu\text{M}$ : A–D, and 2.0  $\mu\text{M}$ : E–H) and PC:PG (1:1) + 10% Cholesterol bilayers (1.25  $\mu\text{M}$ : I–L). Images (A, E and I) show resulting surface topology after 5 min Smp24 incubation whilst (B, F and J) show the topology after 15 min. (C, G and K): Zoomed images of the defects created by Smp24 for the respective bilayer/Smp24 concentrations. (D, H and L): Line profiles across defects for the respective bilayer/Smp24 concentrations (dashed lines across the AFM images illustrate where the profiles were taken).

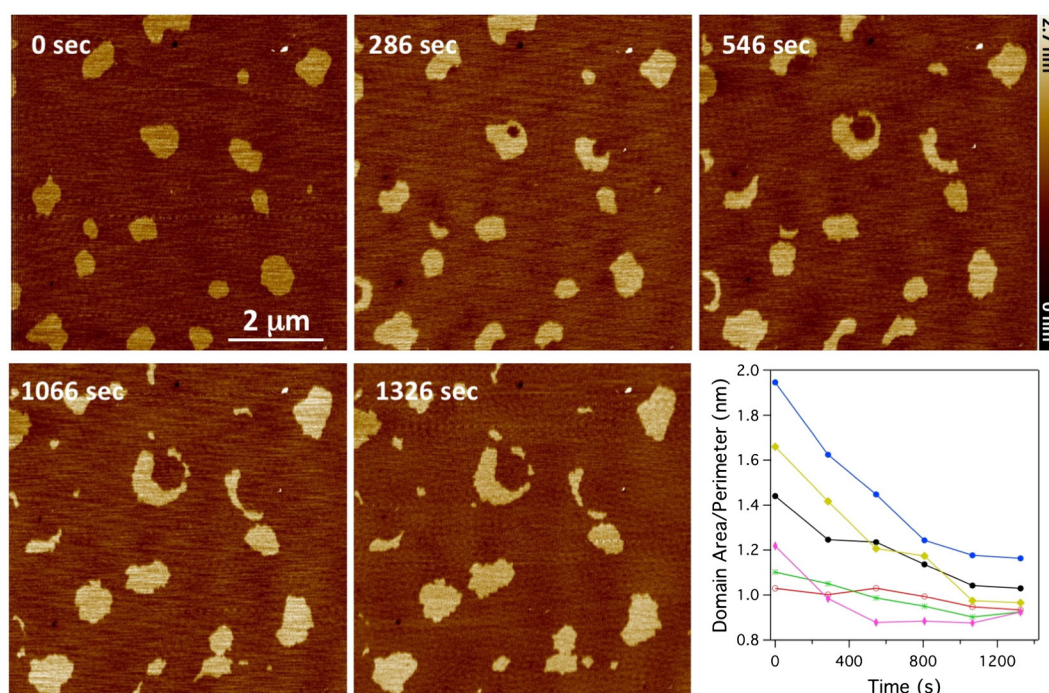


**Fig. 4.** The effect of 1  $\mu$ M Smp24 incubation on phase separated bilayers. 1  $\mu$ M Smp24 was added immediately after capturing the image at time = 0 s. All times shown are at time of full image capture (image scan line rate = 1.97 Hz, 512 lines). Inset graph showing area/perimeter ratios as a functions of time for individual domains.

phospholipids (PG, PS and CR); in comparison eukaryotic membranes mainly consist of the zwitterionic species (PC, PE, and SM) [22]. Although a number of bacteria do contain PE, for example the outer membrane of *E. coli* is predominantly PE [23,24], the membrane compositions chosen within this study reflect prototypical prokaryotic and eukaryotic membranes [24,25]. Smp24 exhibits a membrane disruptive effect on all membrane compositions which is consistent with its antimicrobial and cytotoxic effects [19].

A major driving force of AMP selectivity is the electrostatic attraction to prokaryotic membranes [25,26] which is demonstrated by the inability of Smp24 to disrupt PC:PG liposomes in the presence of 500 mM NaCl. In contrast, no significant salt disruption is seen against the zwitterionic bilayer. PE induces negative curvature of the bilayer, resulting in packing defects [26,27] and a number of peptides (see for example  $\alpha$ -synuclein [27,28] and amphipathic lipid packing sensor (ALPS) motifs such as synapsin 1 [29,30] and ArfGAP1 [31] interact with membranes through a process of curvature-sensing. This phenomenon is thought to be critical to a number of fundamental transport and signalling pathways allowing peptides to identify the correct sub-cellular membrane [31,32]. Upon interaction with the PE containing bilayer Smp24 causes significant rearrangement of the bilayer however no significant accumulation is observed and we postulate that unlike against the PC:PG bilayer where electrostatic attraction and a large peptide concentration is required, relatively few Smp24 molecules may engage in curve sensing, causing such a dramatic bilayer rearrangement.

Whilst electrostatic attraction and lipid defect sensing may be responsible for initial attraction to the PC:PG and PC:PE membrane surface respectively our data suggests that the precise nature of peptide induced membrane disruption is dependent on lipid composition. Pores of varying size are observed in the PC:PG bilayer with liposome leakage data suggesting that complete membrane collapse is not taking place supporting pore formation over a carpet mechanism [8]. Also, the QCM-D data supports this with increased peptide accumulation (decrease in frequency), and increased dissipation, consistent with peptide induced membrane disruption [33]. The dissipation “swing-back” event could result from the threshold peptide concentration being overcome and peptide

molecules mixing with the bilayer, resulting in a reduced interaction with the aqueous phase. This data suggests that Smp24 follows the classical pattern of AMP pore formation, namely (i) electrostatic attraction, (ii) accumulation and (iii) insertion after reaching a critical threshold concentration [30,31]. Our data indicates Smp24 induced pores that are toroidal in nature on the basis of the presence of pores of varying size as peptide concentration increases, leading to complete destruction of the bilayer, as opposed to increased pore formation also the observation of a Smp24 induced decrease in line tension within the *Lo* areas observed during interaction with the phase separated bilayer. This phenomenon has been noted with different membrane-active peptides as examples, PG-1 interacts with the edges of the bilayer and adopts an extended hair pin shape, in which the hydrophilic N-terminus interacts with phospholipid head groups within the bottom leaflet, and the central hydrophilic region interacts with the top leaflet, flanked by two hydrophobic regions sitting within the phospholipid chains [14]. Similarly alpha-helix 5 of the proapoptotic bax peptide, forms pores the mitochondrial cell wall via a toroidal mechanism, as evidenced by a loss of line integrity observed around once-smooth *Lo* areas [34,35].

The mechanism against PC:PE bilayers is radically different, with the formation of stratifications along with phase segregation (Fig. 3A–H). Liposomal leakage is also less marked than with PC:PG suggesting a carpet model is not the primary mechanism. This viewpoint is supported by the QCM-D results which suggest no accumulation event occurs (Fig. 5B). A number of AMPs have previously been shown to disrupt membranes by peptide-mediated non-lamellar formation, suggested as a mechanism of protein-membrane interaction [35,36]. Membrane lipids can self-assemble into different phases, including micellar, lamellar, hexagonal and cubic phases with the ability of membranes to form these structures governed by lipid composition [35,36]. Membranes composed of lipids with a similar headgroup and acyl chain cross sectional area (i.e. PC and PG) favour the formation of planar lipid bilayers, whereas membranes containing PE lipids prefer inverted micelles, inverted hexagonal lipid phases or regions with high negative membrane curvature strain [36,37]. In the absence of peptides, the stored curvature elastic energy causes the bilayer to expand laterally; this



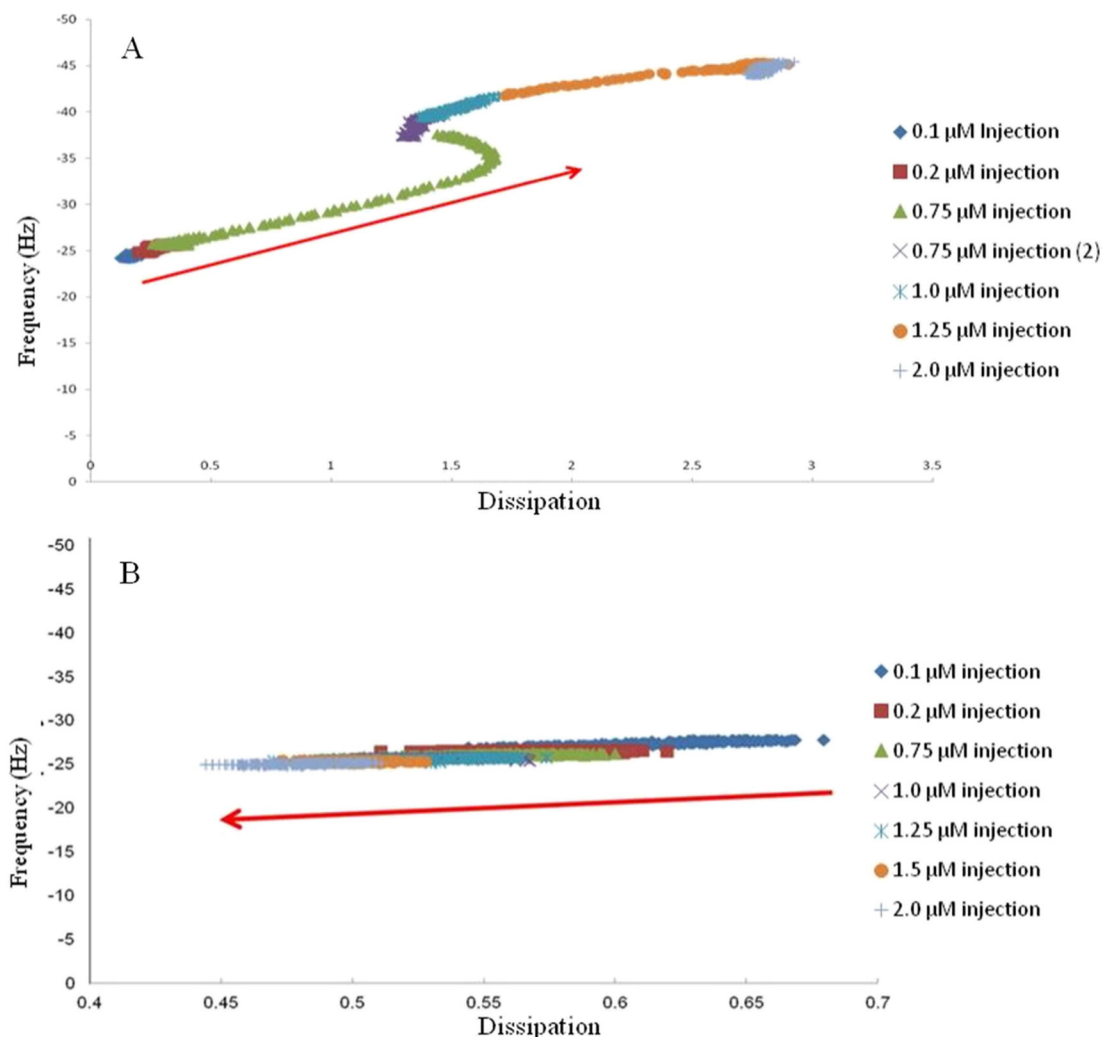


**Fig. 5.** QCM-D analysis of consecutive injections of increasing peptide concentrations (0.2–2  $\mu$ M) against both a PCPG and PCPE bilayer. The red arrow indicates the overall direction of change. (A): Against the PCPG bilayer the bilayer becomes increasingly fluid throughout the time course of the experiment with an increase in peptide interaction with the bilayer, (B): Against a PCPE bilayer a slight decrease in fluidity is observed throughout the time course of the experiment with no peptide accumulation observed.

expansion decreases steric hindrance and is thermodynamically favourable. However, expansion can only occur up to a certain threshold, as changes in membrane conformation cause increased exposure of the acyl chains to water. Consequently beyond this threshold it becomes thermodynamically favourable for an inverse phase to occur. Typically with PE, a hexagonal II phase (HII) tubular structure forms, with the head groups orientated toward the centre of the cylinder, due to its favoured negative curvature. A similar feature was observed for some integral membrane proteins, which may release locally stored curvature elastic stress during protein insertion into the bilayer by allowing the phospholipid chains to dislocate more and forcing head groups together, making the peptide–lipid assembly thermodynamically more stable [36,37]. Lipid lateral stress can be induced by proteins causing membrane structural changes [37–41] and this has suggested a link between alterations in lipid structure and the modification of cell signalling [41,42]. The areas of disruption that occur after Smp24 exposure, seen in the PC:PE bilayer, have a width of between 200 and 350 nm, depending on AMP concentration. However not all the bilayer is removed, with elongated stratifications remaining. Based on the propensity of PE containing bilayers to form non-lamellar phases, Smp24 may induce this process and the stratifications may be elongated structures of non lamellar phase lipids. Several other AMPs (e.g. gramicidin S [42–44], lactoferrin [44,45] sporegrin-1, PGLa and nisin) have been

shown to form non-lamellar structures in PE containing membranes [45–47]. Linear and cyclic arginine- and tryptophan-rich AMPs have been shown to induce de-mixing of a DPPG:DPPE bilayer into separate domains [47]. AMPs with a high positive net charge, conformational flexibility and sufficient hydrophobicity have been shown to facilitate preferential interaction with anionic lipids and the promotion of lipid lateral segregation [48] This mechanism has also been associated with species-specific antimicrobial activity [40,41,49,50].

The inclusion of cardiolipin into the PC:PG bilayer increased the lytic activity of Smp24, but it is not a prerequisite for increased antimicrobial activity. For example, cardiolipin inhibits the pore forming ability of daptomycin in PG liposomes at concentrations of 10 and 20% [50].

## 5. Concluding remarks

This study has evaluated the membrane disruptive effects of a scorpion venom AMP (Smp24) and has provided direct evidence of the same peptide having multiple mechanisms of action depending on the membrane lipid composition. Most AMPs, will to some degree, cause undesirable membrane disruptive effects because they exploit the fundamental biophysical parameters that govern cell membrane–protein interactions. By understanding the precise mechanism by which a single peptide interacts with multiple membrane models, we are better able to

correlate biophysical and biological studies. This will improve our ability to assess the potential of a peptide for having a desirable therapeutic index and to determine if an AMP may interact in a non-lytic fashion with a membrane which could, in turn, disrupt membrane-mediated trafficking and cell signalling events. A better understanding of these processes will ultimately allow us to engineer AMPs which have minimal undesirable effects and hasten their development into clinical use.

### Conflict of interest statement

- (1) This work was funded by a Sheffield Hallam University PhD studentship fund managed by the Biomolecular Science Research Centre.
- (2) There are no financial relationships with any entities that could be viewed as relevant to the general area of the submitted manuscript.
- (3) There were no sources of revenue with relevance to the submitted work who made payments to us or to our institution on your behalf, in the 36 months prior to submission.
- (4) There have been no interactions with the sponsor outside of the submitted work.
- (5) There are no relevant patents or copyrights attached to this study.
- (6) There are no other relationships or affiliations that may be perceived by readers to have influenced, or give the appearance of potentially influencing, what we wrote in the submitted work.

### Transparency document

The Transparency document associated with this article can be found, in online version.

### References

- [1] V. Teixeira, M.J. Feio, M. Bastos, Role of lipids in the interaction of antimicrobial peptides with membranes, *Prog. Lipid Res.* 51 (2) (2012) 149–177.
- [2] H.W. Huang, Action of antimicrobial peptides: two-state model, *Biochemistry* 39 (29) (2000) 8347–8352.
- [3] Y. Shai, Mechanism of the binding, insertion and destabilization of phospholipid bilayer membranes by alpha-helical antimicrobial and cell non-selective membrane-lytic peptides, *Biochim. Biophys. Acta* 1462 (1–2) (1999) 55–70.
- [4] M.N. Melo, R. Ferre, M.A. Castanho, Antimicrobial peptides: linking partition, activity and high membrane-bound concentrations, *Nat. Rev. Microbiol.* 7 (3) (2009) 245–250.
- [5] G. Ehrenstein, H. Lecar, Electrically gated ionic channels in lipid bilayers, *Q. Rev. Biophys.* 10 (1977) 1–34.
- [6] R.E. Hancock, Host defence (cationic) peptides: what is their future clinical potential? *Drugs* 57 (4) (1999) 469–473.
- [7] Y. Park, K.S. Hahm, Antimicrobial peptides (AMPs): peptide structure and mode of action, *J. Biochem. Mol. Biol.* 38 (5) (2005) 507–516.
- [8] O.S. Belokoneva, E. Villegas, G. Corzo, L. Dai, T. Nakajima, The haemolytic activity of six arachnid cationic peptides is affected by the phosphatidylcholine-to-sphingomyelin ratio in lipid bilayers, *Biochim. Biophys. Acta* 1617 (1–2) (2003) 22–30.
- [9] S. Bobone, D. Roversi, L. Giordano, M. Zotti, F. Formaggio, C. Toniolo, Y. Park, L. Stella, Lipid dependence of antimicrobial peptide activity is an unreliable experimental test for different pore models, *Biochemistry* 51 (51) (2012) 10124–10126.
- [10] K. El Kirat, S. Morandat, Y.F. Dufrene, Nanoscale analysis of supported lipid bilayers using atomic force microscopy, *Biochim. Biophys. Acta* 1798 (4) (2010) 750–765.
- [11] A. Won, M. Khan, S. Gustin, A. Akpawu, D. Seebun, T.J. Avis, B.O. Leung, A.P. Hitchcock, A. Ianoul, Investigating the effects of L- to D-amino acid substitution and deamidation on the activity and membrane interactions of antimicrobial peptide anoplins, *Biochim. Biophys. Acta* 1808 (6) (2011) 1592–1600.
- [12] D.I. Fernandez, A.P. Le Brun, T.C. Whitwell, M.A. Sani, M. James, F. Separovic, The antimicrobial peptide aurein 1.2 disrupts model membranes via the carpet mechanism, *Phys. Chem. Chem. Phys.* 14 (45) (2012) 15739–15751.
- [13] K.L. Lam, Y. Ishitsuka, Y. Cheng, K. Chien, A.J. Waring, R.I. Lehrer, K.Y. Lee, Mechanism of supported membrane disruption by antimicrobial peptide protegrin-1, *J. Phys. Chem. B* 110 (42) (2007) 21282–21286.
- [14] K.L. Lam, H. Wang, T.A. Siaw, M.R. Chapman, A.J. Waring, J.T. Kindt, K.Y. Lee, Mechanism of structural transformations induced by antimicrobial peptides in lipid membranes, *Biochim. Biophys. Acta* 1818 (2) (2012) 194–204.
- [15] A. Mularski, J.J. Wilksch, E. Hanssen, R.A. Strugnell, F. Separovic, Atomic force microscopy of bacteria reveals the mechanobiology of pore forming peptide action, *Biochim. Biophys. Acta* 1858 (6) (2016) 1091–1098.
- [16] P.L. Harrison, M.A. Abdel-Rahman, K. Miller, P.N. Strong, Antimicrobial peptides from scorpion venoms, *Toxicon* 88 (2014) 115–137.
- [17] K. Luna-Ramirez, M.A. Sani, J. Silva-Sanchez, J.M. Jimenez-Vargas, F. Reyna-Flores, K.D. Winkel, C.E. Wright, L.D. Possani, F. Separovic, Membrane interactions and biological activity of antimicrobial peptides from Australian scorpion, *Biochim. Biophys. Acta* 1838 (9) (2013) 2140–2148.
- [18] M.A. Abdel-Rahman, V. Quintero-Hernandez, L.D. Possani, Venom proteomic and venomous glands transcriptomic analysis of the Egyptian scorpion *Scorpio maurus palmatus* (Arachnida: Scorpionidae), *Toxicon* 74 (2013) 193–207.
- [19] P.L. Harrison, M.A. Abdel-Rahman, P.N. Strong, M.N. Tawfik, K. Miller, Characterisation of three alpha-helical antimicrobial peptides from the venom of *Scorpio maurus palmatus*, *Toxicon* 117 (2016) 30–36.
- [20] G.R. Heath, B.R. Johnson, P.D. Olmsted, S.D. Connell, S.D. Evans, Actin assembly at model-supported lipid bilayers, *Biophys. J.* 105 (10) (2013) 2355–2365.
- [21] S.D. Connell, G. Heath, P.D. Olmsted, A. Kisil, Critical point fluctuations in supported lipid membranes, *Faraday Discuss.* 161 (2013) 91–111.
- [22] M.R. Yeaman, N.Y. Yount, Mechanisms of antimicrobial peptide action and resistance, *Pharmacol. Rev.* 55 (1) (2003) 27–55.
- [23] C. Ratledge, E.S.G. Wilkinson, *Microbial Lipids*, third ed., Academic Press, London, 1988.
- [24] R.F. Epand, P.B. Savage, R.M. Epand, Bacterial lipid composition and the antimicrobial efficacy of cationic steroid compounds (Ceragenins), *Biochim. Biophys. Acta* 1768 (10) (2007) 2500–2509.
- [25] R.E. Hancock, Peptide antibiotics, *Lancet* 349 (9049) (1997) 418–422.
- [26] L. Vamparys, R. Gautier, S. Vanni, W.F. Bennett, D.P. Tieleman, B. Antonny, C. Etchebest, P.F. Fuchs, Conical lipids in flat bilayers induce packing defects similar to that induced by positive curvature, *Biophys. J.* 104 (2013) 585–593.
- [27] G. Drin, B. Antonny, Amphipathic helices and membrane curvature, *FEBS Lett.* 584 (2010) 1840–1847.
- [28] M.M. Ouberaï, J. Wang, M.J. Swann, C. Galvagnion, T. Guillems, C.M. Dobson, M.E. Welland,  $\alpha$ -Synuclein senses lipid packing defects and induces lateral expansion of lipids leading to membrane remodeling, *J. Biol. Chem.* 288 (29) (2013) 20883–20895.
- [29] L. Krabben, A. Fassio, V.K. Bhatia, A. Pechstein, F. Onofri, M. Fadda, M. Messa, Y. Rao, O. Shupliakov, D. Stamou, F. Benfenati, V. Haucke, Synapsin I senses membrane curvature by an amphipathic lipid packing sensor motif, *J. Neurosci.* 31 (49) (2011) 18149–18154.
- [30] J. Bigay, J.F. Casella, B. Antonny, ArfGAP1 responds to membrane curvature through the folding of a lipid packing sensor motif, *EMBO J.* 24 (2004) 2244–2253.
- [31] B. Antonny, Mechanisms of membrane curvature sensing, *Annu. Rev. Biochem.* 80 (2011) 101–123.
- [32] M. Zasloff, Antimicrobial peptides of multicellular organisms, *Nature* 415 (70) (2002) 389–395.
- [33] G.A. McCubbin, S. Praporski, S. Piantavigna, D. Knappe, R. Hoffmann, J.H. Bowie, F. Separovic, L.L. Martin, QCM-D fingerprinting of membrane-active peptides, *Eur. Biophys. J.* 40 (4) (2011) 437–446.
- [34] A.J. Garcia-Saez, S. Chiantia, J. Salgado, P. Schwille, Pore formation by a Bax-derived peptide: effect on the line tension of the membrane probed by AFM, *Biophys. J.* 93 (1) (2007) 103–112.
- [35] E.F. Haney, S. Nathoo, H.J. Vogel, E.J. Prenner, Induction of non-lamellar lipid phases by antimicrobial peptides: a potential link to mode of action, *Chem. Phys. Lipids* 163 (2010) 82–93.
- [36] G. Tresselt, The multiple faces of self-assembled lipidic systems, *PMC Biophys.* 2 (2009) 3–14.
- [37] W.T. Heller, K. He, S.J. Ludtke, T.A. Harroun, H.W. Huang, Effect of changing the size of lipid headgroup on peptide insertion into membranes, *Biophys. J.* 73 (1997) 239–244.
- [38] K. Lohner, A. Latal, G. Degovics, P. Garidel, Packing characteristics of a model system mimicking cytoplasmic bacterial membranes, *Chem. Phys. Lipids* 111 (2001) 177–192.
- [39] B. Pozo Navas, K. Lohner, G. Deutsch, E. Sevcik, K.A. Riske, R. Dimova, et al., Composition dependence of vesicle morphology and mixing properties in a bacterial model membrane system, *Biochim. Biophys. Acta (BBA)* 1716 (2005) 40–48.
- [40] R.M. Epand, S. Rotem, A. Mor, B. Berno, R.F. Epand, Bacterial membranes as predictors of antimicrobial potency, *J. Am. Chem. Soc.* 130 (2008) 14346–14352.
- [41] R.M. Epand, Lipid polymorphism and protein-lipid interactions, *Biochim. Biophys. Acta Rev. Biomembr.* 1376 (1998) 353–368.
- [42] E.J. Prenner, R.N.A.H. Lewis, R.N. McElhaney, The interaction of the antimicrobial peptide gramicidin S with lipid bilayer model and biological membranes, *Biochim. Biophys. Acta (BBA)* 1462 (1999) 201–221.
- [43] E.J. Prenner, R.N.A.H. Lewis, K.C. Neuman, S.M. Gruner, L.H. Kondejewski, R.S. Hodges, Nonlamellar phases induced by the interaction of gramicidin S with lipid bilayers. A possible relationship to membrane-disrupting activity, *Biochemistry* 36 (1997) 7906–7916.
- [44] D. Zweglick, S. Tumer, S.E. Blondelle, K. Lohner, Membrane curvature stress and antibacterial activity of lactoferricin derivatives, *Biochem. Biophys. Res. Commun.* 369 (2008) 395–400.
- [45] A. Hickel, S. Danner-Pongratz, H. Amenitsch, G. Degovics, M. Rappolt, K. Lohner, Influence of antimicrobial peptides on the formation of nonlamellar lipid mesophases, *Biochim. Biophys. Acta (BBA)* 1778 (2008) 2325–2333.
- [46] S.L. Keller, S.M. Gruner, K. Gawrisch, Small concentrations of alamethicin induce a cubic phase in bulk phosphatidylethanolamine mixtures, *Biochim. Biophys. Acta (BBA)* 1278 (1996) 241–246.



- [47] A. Aroui, M. Dathe, A. Blume, Peptide induced demixing in PG/PE lipid mixtures: a mechanism for the specificity of antimicrobial peptides towards bacterial membranes? *Biochim Biophys Acta (BBA)* (1788) 650–659.
- [48] V. Teixeira, M.J. Feio, L. Rivas, B.G. De la Torre, D. Andreu, A. Coutinho, Influence of lysine Nε-trimethylation and lipid composition on the membrane activity of the cecropin A-melittin hybrid peptide CA(1–7)M(2–9), *J. Phys. Chem. B* 114 (2010) 16198–16208.
- [49] R.M. Epand, R.F. Epand, Lipid domains in bacterial membranes and the action of antimicrobial agents, *Biochim. Biophys. Acta (BBA)* 1788 (2009) 289–294.
- [50] T. Zhang, J.K. Murailh, N. Tishbi, J. Herskowitz, R.L. Victor, J. Silverman, S. Uwumarenogie, S.D. Taylor, M. Palmer, E. Mintzer, Cardiolipin prevents membrane translocation and permeabilization by daptomycin. 2014, *J. Biol. Chem.* 289 (17) (2014) 11584–11591.